ORIGINAL ARTICLE

β-Cyclodextrin-Grafted Cobalt-Aluminum Bimetallic Oxide Modified Acrylic Ester Resin for Oil/Water Separation

Jie Wen[1] · Yanjun Lyu[1] · Lianhong Zhang[1] · Yuling Ma[1] · Xia Huang[2] · Wanyu Zhu[3]

Abstract

A novel method was developed to introduce β-cyclodextrin (β-CD) cage-like macromolecules into acrylic ester resin using metal oxides as a medium, resulting in high-oil-absorption resin composites. β-CD was first grafted onto the surface of cobalt-aluminum bimetallic oxide (CoAl-LDO) via a facile hydrothermal method in an alkaline environment, generating more pore structures. To enhance the hydrophobic properties of β-CD-grafted CoAl-LDO nanoparticles, KH-570 was employed as a modifier to modify nanoparticles. Finally, the β-CD-grafted CoAl-LDO/acrylic ester resin composite was successfully synthesized by suspension polymerization method. The oil absorption performance of the resin composite was evaluated using various solvents. Its saturated capacity reached 18.62 g/g for cyclohexane, 19.92 g/g for toluene, and a remarkable 31.42 g/g for trichloromethane. Even for diesel, a challenging oil due to its viscosity, the absorption reached a noteworthy 16.17 g/g. Further demonstrating its selectivity, the composite strictly adsorbed oil while repelling water. Notably, the impressive capacity remained largely unchanged after eight regeneration cycles.

Keywords Acrylic ester resin · Nanoparticle · β-cyclodextrin · Oil uptake capacity · Reusability

Introduction

High-oil-absorption resin is a new type of functional polymer material with a wide range of oil absorption, high oil–water selectivity, fast oil absorption rate, and good oil retention properties. A common method for modifying resin is to add inorganic nanoparticles. These nanoparticles can significantly reduce the degree of polymerization and weaken the entanglement of chains in the polymer system. Zhang et al. [1] synthesized Mn_2O_3/poly(St-BMA) resin composites using a combination of biological template technology and microwave polymerization. They studied the application of these composites in oil absorption. The

results showed that these composites have good thermal stability and recyclability. Yue et al. [2] developed hierarchical porous Al_2O_3/acrylic resin composites. This hybrid resin can effectively reduce the mass transfer resistance and accelerate the absorption of oil and organic solvents. Zhang et al. [3] employed a microwave polymerization route to synthesize Al_2O_3 microspheres/acrylic ester resin hybrids. The resulting resin composite exhibited an excellent reusability. However, the current challenge lies in achieving high-oil-absorption capacity, particularly for real oil, using resins modified by inorganic nanoparticles.

Cyclodextrins (CDs), a common natural polymer derived from starch degradation [4], possess a unique structure resembling a conical toroid with a central cavity. The outer surface of CDs is decorated with hydroxyl groups, exhibiting hydrophilicity, while the interior cavity is hydrophobic. This unique structure grants CDs broad applicability in various fields, including drug delivery [5, 6], absorption [7, 8], and catalysis [9, 10]. Among cyclodextrins, β-cyclodextrin (β-CD) is particularly attractive due to its affordability and ready availability [11]. Inheriting the advantages of CDs mentioned above, β-CD has gained significant interest in the production of adsorbents [12–15]. Ding et al. [16] first synthesized a derivative of β-CD (β-CD-A), which was

---

✉ Lianhong Zhang
zhanglianhong@swpu.edu.cn

1 Oil and Gas Field Applied Chemistry Key Laboratory of Sichuan Province, College of Chemistry and Chemical Engineering, Southwest Petroleum University, Chengdu, China

2 Nanomaterials Centre, Australian Institute of Bioengineering and Nanotechnology, The University of Queensland, Brisbane, Australia

3 Tongwei Solar Energy (Chengdu) Co., Ltd., Chengdu, China

copytymerized with octadecyl acrylate (ODA) and butyl acrylate (BA) to obtain a crosslinked oil-absorbing resin. Oil absorption results indicated that the oil absorbent containing CD groups exhibited higher oil-absorption performance. Additionally, β-CD can participate in polymerization reactions as a comonomer, crosslinker, and pore-forming agent. He et al. [17] successfully prepared high-oil-absorption microspheres containing β-CD through suspension polymerization. These microspheres not only possess a porous structure but also exhibit high oil absorbency and excellent oil retention performance. Unfortunately, existing methods require converting β-CD into costly derivatives and involve complex synthesis process, making it difficult to achieve large-scale production and practical application of absorbents. Therefore, a readily synthesized oil-absorbing resin with superior performance is crucial for this field.

This study introduces a novel approach for creating high-performance oil-absorbent resins without the need for complex synthesis of β-CD derivatives. Instead, β-CD was directly grafted onto cobalt-aluminum bimetallic oxide nanoparticles (CoAl-LDO-ECD) using a facile hydrothermal method. CoAl-LDO-ECD was then modified with KH-570 for surface hydrophobicity and subsequently combined with acrylic ester resin to form the final oil-absorbent material. This design has two advantages: cobalt-aluminum bimetallic oxide (CoAl-LDO) nanoparticles enhance the mechanical strength of the resin composite, while the cage-like β-CD macromolecules improve its pore structure, promoting efficient oil absorption. The prepared resin composite was comprehensively characterized using XRD, FT-IR, CA, SEM, and TG analyses. Furthermore, its oil absorption properties, including oil uptake capacity, oil absorption kinetics, oil–water selectivity, and reusability, were evaluated.

Experimental

Chemical Reagents

Octadecyl methacrylate (SMA), analytical grade, produced by Chengdu Selwyns Bioengineering Co., Ltd.; β-cyclodextrin (β-CD), ethylenediaminetetraacetic acid (EDTA), disodium hydrogen phosphate (Na$_2$HPO$_4$), poly(vinyl alcohol) (PVA), isobutyl methacrylate, 3-methacryloxypropyltrimethoxysilane (KH-570), aluminum nitrate (Al(NO$_3$)$_3$ 9H$_2$O), cobalt nitrate (Co(NO$_3$)$_2$ 6H$_2$O), and sodium hydroxide (NaOH), analytical grade, produced by Aladdin Reagent Co., Ltd.; poly(ethylene glycol)-200 (PEG-200), Sudan III, sodium carbonate (Na$_2$CO$_3$), divinylbenzene (DVB), benzoyl peroxide (BPO), ethyl acetate (EA), ethanol, toluene, cyclohexane, and trichloromethane, analytical grade, produced by Chengdu Keron Chemical

Reagent Factory; diesel fuel purchased from the Sinopec gas station near Southwest Petroleum University.

Synthesis of High-Oil-Absorption Resin Composite

Preparation of Cobalt-Aluminum Bimetallic Oxide

To prepare a cobalt-aluminum double hydroxide (CoAl-LDHs) sol, 10 mmol Na$_2$CO$_3$ was weighed in a 200 mL beaker and dissolved in water. The solution was heated to 65 °C in a constant temperature water bath while stirring. A 1 mol/L NaOH solution was prepared and mixed well. The NaOH solution was then loaded into a burette. In another beaker, 10 mmol Co(NO$_3$)$_2$ 6H$_2$O and 5 mmol Al(NO$_3$)$_3$ 9H$_2$O were weighed and dissolved in water to obtain a certain concentration of salt solution. The salt solution was mixed well and loaded into a burette. Subsequently, the salt solution and NaOH solution were titrated into the Na$_2$CO$_3$ solution in the beaker, controlling the pH value within a certain range. The as prepared mixture was aged at 65 °C for 24 h to obtain a CoAl-LDHs sol. Finally, the CoAl-LDHs sol was filtered and calcined at 500 °C for 4 h to gain CoAl-LDO nanoparticles.

Grafting of Cobalt-Aluminum Bimetallic Oxides with β-Cyclodextrin

In a 0.01 mol/L NaOH solution, a certain amount of β-CD and CoAl-LDO powder was dissolved, and PEG-200 was added as a dispersant. The mixture was ultrasonically dispersed for 30 min to make it uniformly mixed. In a constant temperature water bath at 60 °C, the mixture was stirred for 1 h, 5 g EDTA was added, and a certain amount of Na$_2$HPO$_4$ was added. The mixture was stirred until a thick sol-like substance was formed in the beaker. Then, the colloidal solution was quickly poured into a polytetrafluoroethylene (PTFE) reactor and reacted at 160 °C for 24 h. The product, named CoAl-LDO-ECD, was washed and dried. The preparation process of CoAl-LDO-ECD is shown in Fig. 1.

Hydrophobic Modification

In a system of anhydrous ethanol/deionized water (volume ratio of 1:1), 1 g CoAl-LDO-ECD powder was added and ultrasonically dispersed to make it uniformly dispersed. A certain amount of KH-570 solution was added and stirred at 85 °C for 6 h. After centrifugation, washing, and drying, CoAl-LDO-ECD-KH was obtained. The modification process of CoAl-LDO-ECD is illustrated in Fig. 1.

Fig. 1 Schematic diagram of high-oil-absorption resin synthesis process
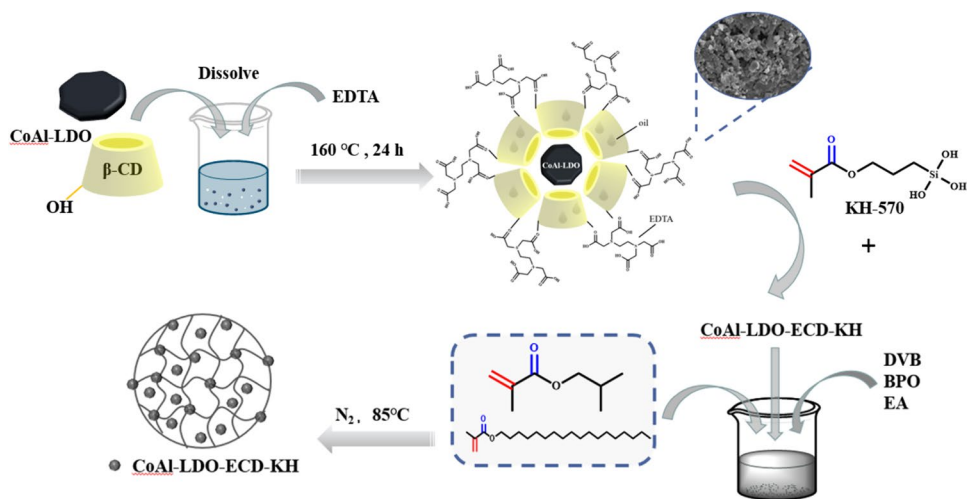
Synthesis of Resin Composite

A certain amount of PVA was dissolved in a beaker, heated to 90 ℃ to fully swell. After cooling to 40 °C, it was poured into a 250 mL flask and purged with N_2 to remove air. Then, the mixture of copolymer monomers SMA, isobutyl methacrylate, DVB, BPO, EA, and CoAl-LDO-ECD-KH was added, and heated to 85 °C to synthesize resin composite. After reacting for 4 h, it was filtered, and washed with deionized water and ethanol. Finally, the product was put in a Soxhlet extractor for purification for 24 h, and dried in a drying oven at 60 °C for 3 days. The synthesis process of resin composite is shown in Fig. 1.

Oil Absorption Performance

Oil Uptake Capacity

The experiment to measure the oil uptake capacity of resin in the test oil is carried out at room temperature using a weight measurement method. The polyester non-woven bag and about 1 g of dried absorbent resin are weighed, and the resin was placed in the polyester non-woven bag. The polyester non-woven bag is immersed in the oil or organic solvent for saturated absorption (12 h) and sealed with plastic wrap to prevent evaporation of the liquid. After the resin has finished the absorption, the polyester non-woven bag is removed and dripped for a few minutes until there are no residual oil droplets on the bag surface. It is then reweighed. The oil absorption experiment is repeated three times each time, and the average value is taken. The oil uptake capacity of the resin is calculated using the following formula:

$$Q = \frac{m_2 - m_1 - m_0}{m_0}. \tag{1}$$

In the formula, Q is the oil uptake capacity of the resin, g/g; m_0 is the weight of the resin, g; m_1 is the weight of the polyester non-woven bag, g; m_2 is the total weight of the resin and bag after absorbing oil, g.

Oil Absorption Rate

The absorption rate of resin to the test oil can also be measured using a weight measurement method. The polyester non-woven bag and dried resin (about 1 g) are weighed. The resin is placed in the polyester non-woven bag and immersed in the oil or organic solvent. The oil is absorbed for a certain period. Then, the bag is removed and allowed to drip for a few minutes until there are no residual oil droplets on the surface. The bag is weighed again and the weight is recorded. The oil uptake capacity under different absorption time is calculated by formula (1).

Oil–Water Selectivity

A certain amount of trichloromethane, cyclohexane, toluene, or diesel fuel was weighed into a beaker containing a certain amount of aqueous solution. The oil was dyed with Sudan III. Then, the resin was added to above mixture and the absorption of oil by the resin was observed. The operation was carried out at room temperature for 6 h. Finally, the resin was filtered out and weighed to obtain the oil uptake capacity of the resin in the oil–water mixture.

Regeneration Performance

To regenerate resin using ethanol extraction, resin saturated with trichloromethane is selected. First, the synthesized resin is immersed in trichloromethane until saturation absorption is reached. Second, the saturated resin is immersed in a certain amount of ethanol to release the adsorbed oil (multiple

times), completing the desorption process. Finally, the desorbed resin is placed in an oven to dry. The oil absorption–oil desorption process is repeated eight times to determine the resin reusability. The resin is weighed before and after each cycle.

Characterization of Resin

Fourier Transform Infrared Spectroscopy (FT-IR)

A WQF520 infrared spectrometer (Beijing Riley Analytical Instrument Co., Ltd.) was used to characterize the structure of CoAl-LDO-ECD before and after modification. The test conditions were as follows: CoAl-LDO-ECD before and after hydrophobic modification was ground, dried, and pressed into a pellet, and then placed in an infrared spectrometer for testing (scanning 16 times, wavelength range of 4400–400 cm^{-1}).

X-Ray Diffraction Analysis (XRD)

A PANalytical X'Pert Pro MPD X-ray diffractometer was used to characterize the phase composition of CoAl-LDO-ECD and CoAl-LDO-ECD-KH. The test conditions were as follows: Cu target, Kα radiation, scanning range $2\theta = 5 \sim 70°$. The samples were ground into particles of about 10 μm in diameter, transferred to the sample holder, and gently flattened with a glass slide to a thickness of 2 mm.

Scanning Electron Microscopy (SEM)

To observe the morphology and particle size of the materials, a Zeiss GeminiSEM300 field-emission SEM (Carl Zeiss, Germany) was used.

Static Contact Angle Analysis (CA)

An SDC-200S contact angle tester (Shen Ding Co., Ltd., Dongguan, China) was used to measure the static contact angle of both CoAl-LDO-ECD and CoAl-LDO-ECD-KH particles, allowing for a comparison of their wetting behaviors. The samples were dried and then pressed into pellets for testing. Deionized water was used to drop on the samples, and the CA values were obtained.

Thermogravimetric Analysis (TG)

A TGA/DSC 3+ thermal analyzer (Mettler-Toledo International, Switzerland) was used to characterize the thermal stability of the resin. The tests were conducted under a nitrogen atmosphere, with a gas flow rate of 100 mL/min and a heating rate of 10 °C/min, from 30 to 800 °C.

Results and Discussion

XRD Analysis

Figure 2a shows the XRD spectra of CoAl-LDO-ECD before and after hydrophobic modification. The results show that the peaks at $2\theta = 31.12°$ and $36.5°$ correspond to the (220) and (311) planes of $CoAl_2O_4$ (PDF#38-0814).
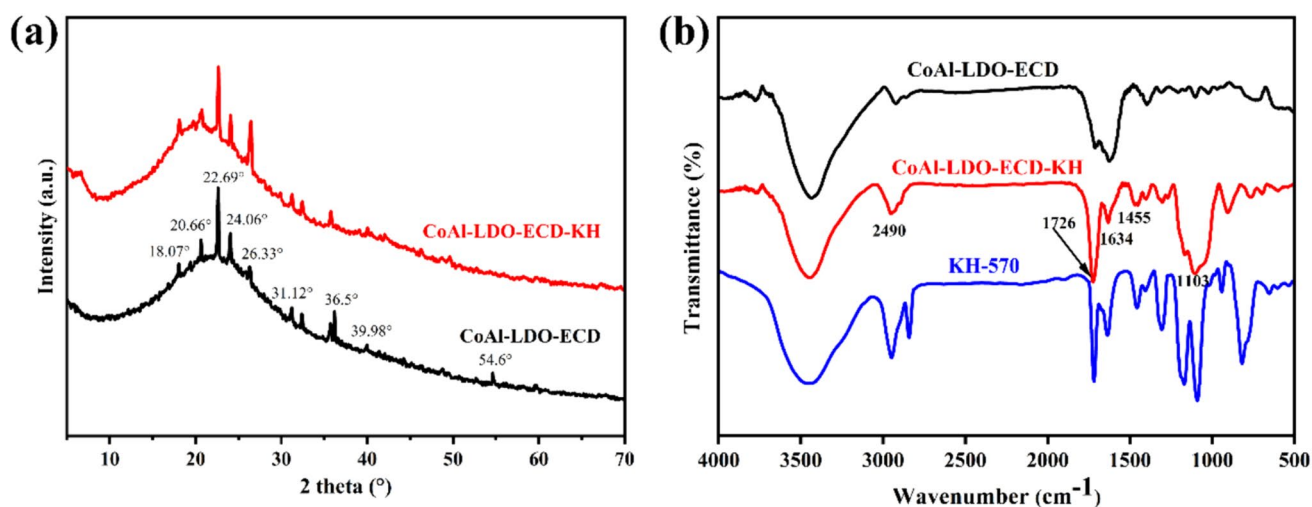

Fig. 2 **a** XRD spectra of CoAl-LDO-ECD before and after hydrophobic modification; **b** FT-IR spectra of CoAl-LDO-ECD, CoAl-LDO-ECD-KH, and KH-570

The diffraction peaks at 2θ = 18.07° and 20.66° belong to β-CD [18, 19]. The diffraction peak at 2θ = 24.06° is indicative of EDTA [20]. These characteristic diffraction peaks indicate that β-CD and EDTA exist in CoAl-LDO-ECD. Furthermore, these characteristic diffraction peaks confirm that β-CD has been successfully grafted to the surface of CoAl-LDO nanoparticles. At the same time, it can also be seen from the figure that the diffraction peaks of CoAl-LDO-ECD before and after hydrophobic modification have hardly changed, indicating that the crystal structure of CoAl-LDO-ECD will not be changed by the chemical modification of KH-570.

FT-IR Analysis

To further understand whether the hydrophobic modification of CoAl-LDO-ECD is successful, FT-IR was used to characterize CoAl-LDO-ECD and CoAl-LDO-ECD-KH, and the results are shown in Fig. 2b. From Fig. 2b, it can be seen that CoAl-LDO-ECD-KH, which has been hydrophobically modified by KH-570, has the characteristic absorption peaks of both CoAl-LDO-ECD and KH-570. Among them, the spectrum of CoAl-LDO-ECD-KH has an absorption peak of C–H-stretching vibration at 2940 cm^{-1} [20], an absorption peak of C=O-stretching vibration at 1726 cm^{-1} [19], an absorption peak of C=C-stretching vibration at 1634 cm^{-1} [21], an absorption peak of −CH$_2$-bending vibration at 1455 cm^{-1} [22], and a characteristic absorption peak of

Si–O–Si or Si–O bonds at 1103 cm^{-1} [23]. These characteristic absorption peaks indicate that the organic groups in KH-570 have been successfully grafted onto the surface of the CoAl-LDO-ECD substrate. This successful modification introduces hydrophobic characteristics to the resulting CoAl-LDO-ECD-KH composite material, thereby altering its surface properties.

CA Analysis

To test the hydrophobicity of CoAl-LDO-ECD and CoAl-LDO-ECD-KH, the contact angles of the two materials were measured using the static water drop method. The test results are shown in Fig. 3. As shown in Fig. 3, CoAl-LDO-ECD has a significant difference in wettability to water before and after hydrophobic modification with KH-570. As shown in Fig. 3a, when deionized water droplets fall on the surface of CoAl-LDO-ECD powder, the droplets collapse in a very short time. The contact angle of CoAl-LDO-ECD is 14.59°, indicating that the surface of CoAl-LDO-ECD is highly hydrophilic. Conversely, as shown in Fig. 3b, the water droplets remain in a spherical shape on the surface of CoAl-LDO-ECD-KH powder, and have a stable contact angle of 139.95°. CoAl-LDO-ECD-KH is in a clear hydrophobic state, indicating that hydrophobic groups have been successfully grafted to the surface of CoAl-LDO-ECD. Figure 3c and d shows high-definition images of the hydrophobicity tests of CoAl-LDO-ECD and CoAl-LDO-ECD-KH.

Fig. 3 Static contact angles of **a** CoAl-LDO-ECD and **b** CoAl-LDO-ECD-KH; high-definition images of the hydrophobicity tests of **c** CoAl-LDO-ECD and **d** CoAl-LDO-ECD-KH
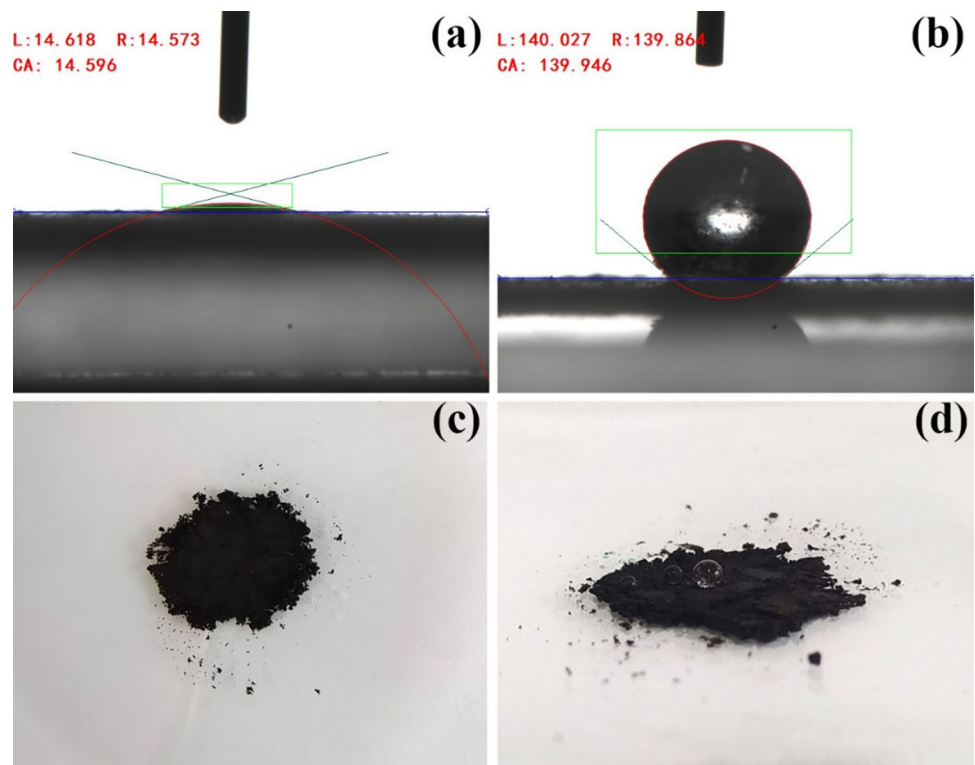
In Fig. 3c, when deionized water droplets fall on the surface of CoAl-LDO-ECD, the droplets completely collapse and spread out. The water droplets in Fig. 3d remain in a small spherical shape on the surface of CoAl-LDO-ECD-KH, and do not deform even as the residence time increases. This further indicates that CoAl-LDO-ECD-KH has good hydrophobicity, which is consistent with the results of the CA test, proving that CoAl-LDO-ECD has been successfully hydrophobically modified.

SEM Analysis

Scanning electron microscopy (SEM) was used to characterize the surface morphology of the synthesized CoAl-LDO-ECD particles and resin composite. Figure 4a–c shows SEM images of CoAl-LDO-ECD at different magnifications. It can be observed from the images that the prepared CoAl-LDO-ECD has a lamellar structure with a diameter of about 500 nm, and the lamellar structure is not uniform. Figure 4d–f shows SEM images of resin composite at different magnifications. It can be observed from the images that the surface of the resin composite is uneven, with many grooves and holes of varying dimensions and depths. These uneven holes and grooves increase the pore volume of the resin composite, expand its contact area with the oil, and make it easier for the oil to diffuse into the resin [17, 24]. The inset in Fig. 4e is a magnified local image of the yellow rectangular box. The white highlights highlighted by the yellow circle in the inset are CoAl-LDO-ECD-KH particles. Figure 4f is a magnified image of CoAl-LDO-ECD-KH. It can be clearly seen that the magnified morphology is lamellar (highlighted in yellow), which indicates that CoAl-LDO-ECD-KH is successfully compounded with resin [8]. In addition, the successful hybridization of CoAl-LDO-ECD-KH with resin

indicates that it participates in the construction of the 3D network structure of the resin and plays a certain supporting role in the network structure of the resin composite, increasing the strength of the resin composite. This unique 3D network structure, combined with the advantages of CoAl-LDO-ECD-KH particles and acrylic resin, is beneficial to improve the absorption capacity of the resin composite for oil.

TG Analysis

Figure 5 shows the thermogravimetric (TG) curves of the raw resin and resin composite. As shown in Fig. 5b, the first stage of thermal loss of the resin composite is from 0 to 327 °C, with a mass loss rate of about 10%, indicating that the thermal stability of the resin composite is good in this stage. The second stage of thermal loss is from 327 to 415.6 °C, with a mass loss rate of about 90%. This is mainly due to the rupture of various cross-linking bonds in the resin, as well as the decomposition of the main and side chains [25]. A strong exothermic peak occurs at 375 °C, corresponding to a mass loss rate of about 95%. This may be related to the melting of the resin composite [26]. The third stage is from 415.6 to 800 °C. After 470 °C, the mass of the resin composite basically does not change. Compared with the final decomposition temperature of the raw resin, the complete decomposition temperature of the resin composite is higher than that of the raw resin. In addition, compared with Fig. 5a, the main weight loss of the raw resin and the resin composite starts at 239 and 327 °C, respectively. The strong exothermic peak and the decomposition temperatures in each stage of the resin composite are all increased to some extent. This indicates that the addition of
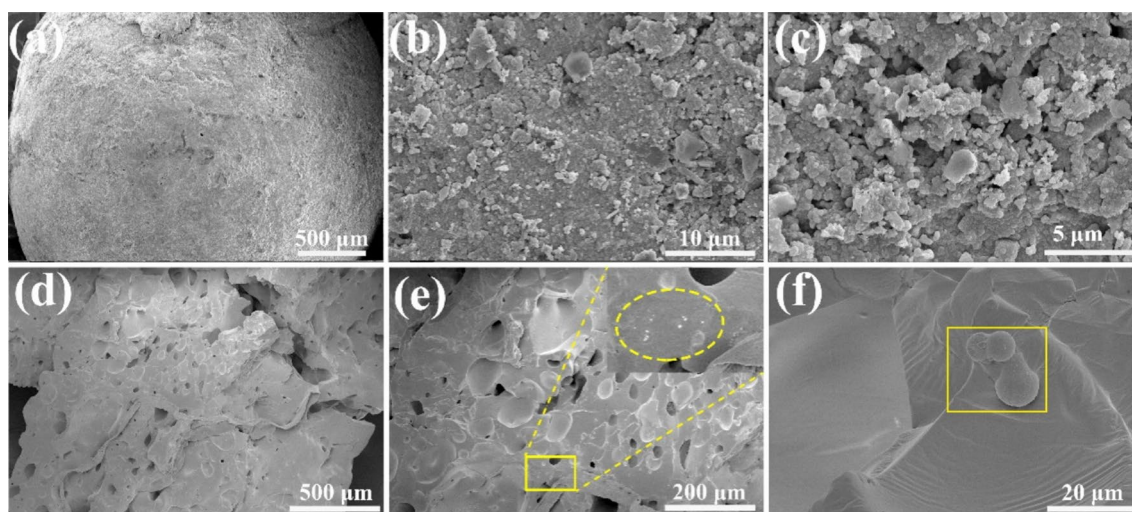

Fig. 4 SEM images of **a**–**c** CoAl-LDO-ECD and **d**–**f** resin composite at different magnification
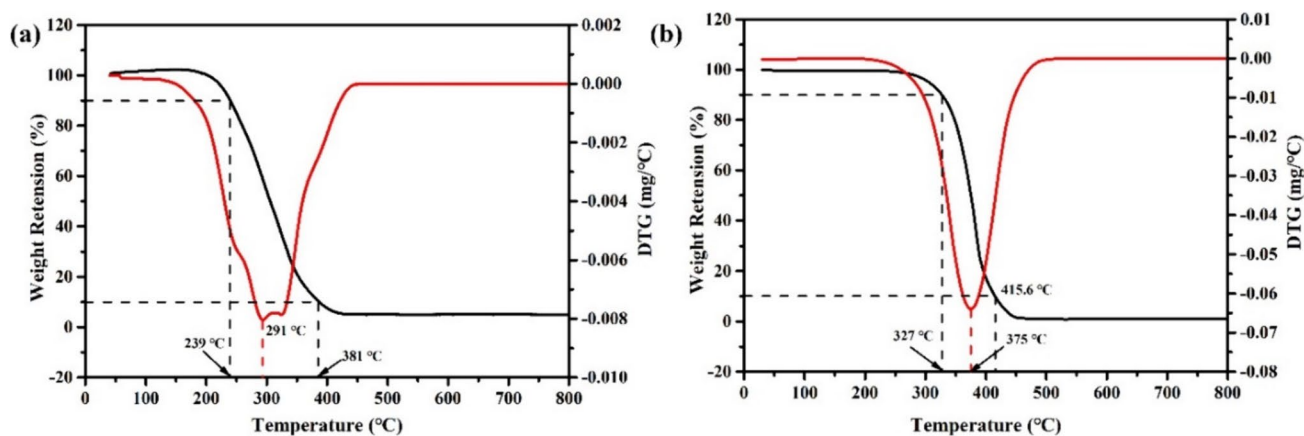
Fig. 5 TG-DTG thermogram of **a** raw resin and **b** resin composite

CoAl-LDO-ECD-KH has improved the thermal stability of the resin composite.

Oil Uptake Capacity

CoAl-LDO-ECD-KH is hydrophobic and can cooperate with the raw resin to absorb oil. At the same time, the hydrophobic groups in CoAl-LDO-ECD-KH nanoparticles can react with polymer chains to cross-link and participate in the construction of a 3D network structure, forming more cross-linking points between CoAl-LDO-ECD-KH and polymer chains [27]. This not only increases the pore structure of the resin composite, but also improves its gel strength. Therefore, the addition amount of CoAl-LDO-ECD-KH affects the oil uptake capacity of the resin composite. The effect of the addition amount of CoAl-LDO-ECD-KH on the uptake capacities of resin composite for trichloromethane, toluene, cyclohexane, and diesel is shown in Fig. 6a. As shown in Fig. 6a, the oil uptake capacity of the resin composite first increases and then decreases with the increase of the addition amount of CoAl-LDO-ECD-KH. The reason for this trend can be explained as follows: when the amount of CoAl-LDO-ECD-KH is too much, the dispersibility of the resin composite will increase, and the resin particles will become smaller, resulting in its 3D network structure being incomplete and the network space being reduced. In addition, CoAl-LDO-ECD-KH occupies the 3D network structure of the resin, reduces the swelling ability of the resin, and hinders the extension of the chain, which is not conducive to the absorption of oil by the resin. Therefore, the maximum oil uptake capacities of the CoAl-LDO-ECD-KH resin composite toward diesel, cyclohexane, toluene, and trichloromethane was achieved at 2 wt% CoAl-LDO-ECD-KH addition, reaching values of 16.17, 18.62, 19.92, and 31.42 g/g, respectively.

The oil absorption performance of the prepared resin composite was compared with that of the oil-absorbing resins containing inorganic nanoparticles reported in recent literature, as shown in Table 1. As can be seen from the table, the resin composite prepared in this work has remarkable oil-absorption uptake capacity, especially for diesel, which is significantly higher than the literature reports. This could be attributed to the gaps formed by the β-CD rings and its hydrophobic pores.

Oil Absorption Kinetics

Figure 6b shows the change trend of the oil uptake capacities of the resin composite with time for the tested oils. As can be seen from the figure, the oil uptake capacities of all four tested oils increase with the increase of the absorption time. The resin composite reaches saturation absorption for trichloromethane, toluene, cyclohexane, and diesel at 90, 120, 150, and 180 min, respectively. Compared with the oil-absorbing resins prepared with β-CD reported in the literature [16, 17, 24], the saturation absorption time of the resin composite is shortened. This shows that the addition of β-CD-grafted CoAl-LDO nanoparticles is beneficial to improve the oil absorption performance of the resin. The pseudo-first-order [31] and pseudo-second-order [32] kinetic models were used to evaluate the absorption process of trichloromethane by the resin composite. Figure 6c and d shows the kinetic model fitting curves of the absorption process of trichloromethane by the resin composite: (c) pseudo-first-order kinetics, and (d) pseudo-second-order kinetics. The corresponding fitting parameters and kinetic correlation coefficients are listed in Table 2. As can be seen from Table 2, the R^2 value of the pseudo-first-order kinetics is significantly different from 1, indicating a weak linear relationship between $\ln(q_e - q_t)$ and t. This shows that the absorption behavior of the resin composite for trichloromethane
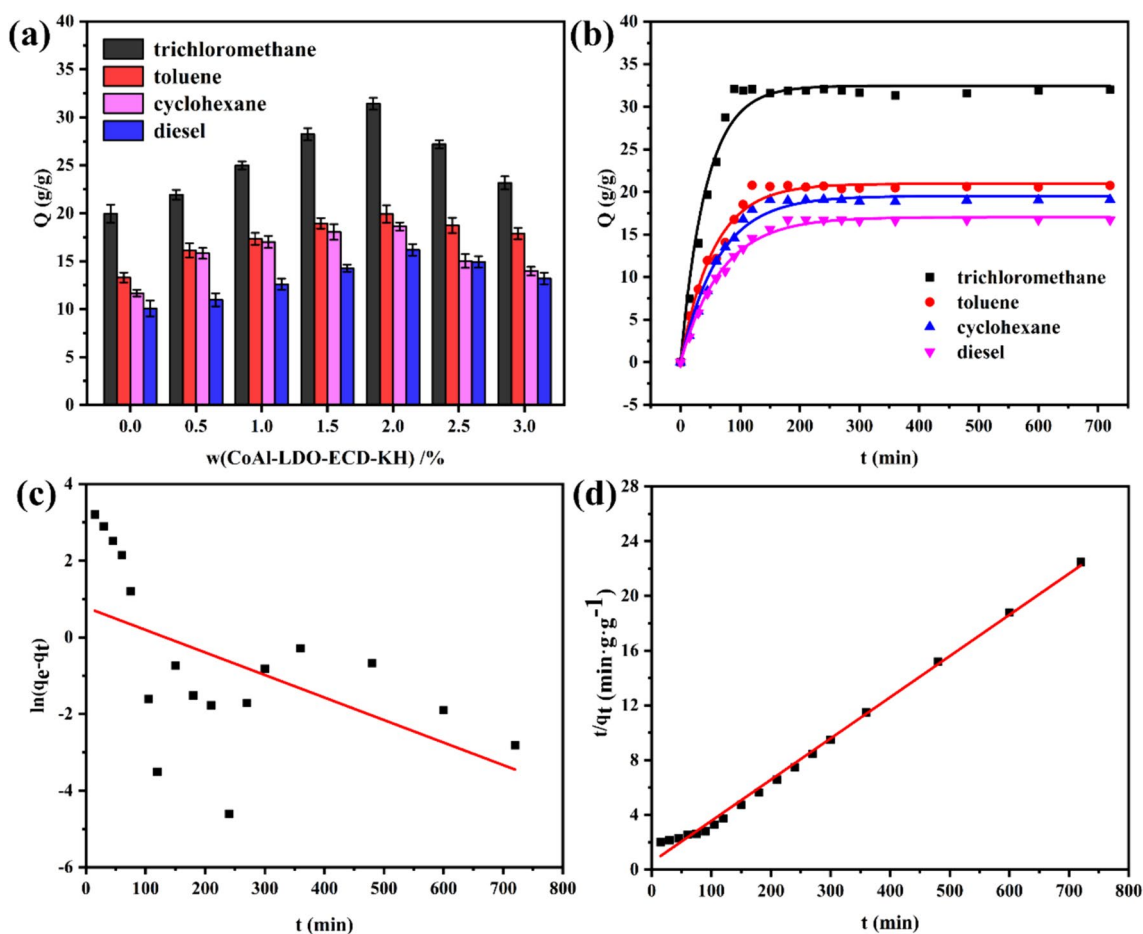
Fig. 6 **a** Effect of CoAl-LDO-ECD-KH addition on the absorbency of resin composite; **b** oil absorption rate of resin composite for the tested oils; **c** pseudo-first-order and **d** pseudo-second-order kinetics of the absorption process of trichloromethane by the resin composite

Table 1 Comparison of oil absorption properties of resins

Materials	Preparation method	Trichloromethane (g/g)	Toluene (g/g)	Cyclohexane (g/g)	Diesel (g/g)	References
Mn$_2$O$_3$/poly(St-BMA) resin composites	Microwave polymerization	/	~15		9.30[a]	[1]
Porous Al$_2$O$_3$/acrylic resin composites	Microwave suspension polymerization	~28	~18	/	/	[2]
Al$_2$O$_3$ microspheres/acrylic ester resin	Microwave polymerization	29.85	/	/	~2.50	[3]
ZnO/acrylic ester resin	Suspension polymerization	30.87	23.56	/	~2.80	[28]
Polyacrylate resin	Suspension polymerization	17.11	12.60	~2.50	/	[29]
Hybrid composite resin	Suspension polymerization	/	20.51	/	7.03	[30]
Raw resin	Suspension polymerization	20.69	13.87	12.05	10.93	This work
Resin composite	Suspension polymerization	31.42	19.92	18.62	16.17	This work

[a]The absorption capacity of gasoline

Table 2 Pseudo-first-order and pseudo-second-order kinetic parameters of absorption of trichloromethane by resin composite

Kinetic model	Equation	k	R^2
Pseudo-first-order	$\ln(q_e - q_t) = \ln(q_e) - k_1 t$	-0.00588 min^{-1}	0.2326
Pseudo-second-order	$t/q_t = 1/(k_2 q_e^2) + t/q_e$	0.03012 g (g min)$^{-1}$	0.9951

does not conform to the pseudo-first-order kinetic model. The R^2 value in the pseudo-second-order kinetic model ($R^2 = 0.9960$) is very close to 1, indicating that the linear fitting is good. At the same time, combined with Fig. 6d, the linear relationship between t/q_t and t in the figure is good, indicating that the absorption process of trichloromethane by the resin composite conforms to the pseudo-second-order kinetic model.

Oil–Water Selectivity

In practical applications, oil absorbent materials are usually used to absorb oil in oil–water mixtures. To verify the oil uptake capacity of the resin composite in oil–water mixtures, the oil absorption performance of the resin composite for the test oils in oil–water mixtures was investigated in this work, as shown in Fig. 7a. As can be seen from Fig. 7a, even in oil–water mixtures, the resin composite has good oil absorption performance for the test oils. Its oil uptake capacities in oil–water mixtures for trichloromethane, toluene, cyclohexane, and diesel are 28.84, 16.86, 16.87, and 13.86 g/g, respectively, which account for 91.79, 84.64, 90.60, and 85.71% of the pure oil uptake capacities. The

reduced oil uptake capacity of the resin composite observed in oil–water mixtures could be attributed to increased diffusional resistance of oil molecules through the water barrier [33].

Reusability of the Resin Composite

The reusability of resin is an important property in practical applications. To evaluate the reusability of the resin composite, this work used trichloromethane as the target oil to test the regeneration performance of the raw and resin composites for eight times, and the results are shown in Fig. 7b. As can be clearly seen from Fig. 7b, the oil removing efficiency of the resin after compounding decreases very slowly with the increase of the number of regenerations. Compared with the raw resin, the oil uptake capacity of the resin composite for trichloromethane increased by about 57.1% in the first cycle. In addition, even after eight cycles of absorption, the oil uptake capacity of the resin composite for trichloromethane can still maintain 88% of the initial value, while the raw resin only maintains 69% of the initial value. On the one hand, it may be because the process of extraction with anhydrous ethanol does not seriously damage the structure of the material; on the other hand, it may also be because the hydrophobic groups in CoAl-LDO-ECD-KH nanoparticles form many cross-linking points with polymer chains, participate in the construction of 3D network structure, and increase the strength of the resin composite. Even after repeated absorption, the chain segments of the resin composite will not dissolve [2]. Additionally, the introduction of β-CD molecules further increases the pore structure of the resin composite [24]. These pores increase the effective
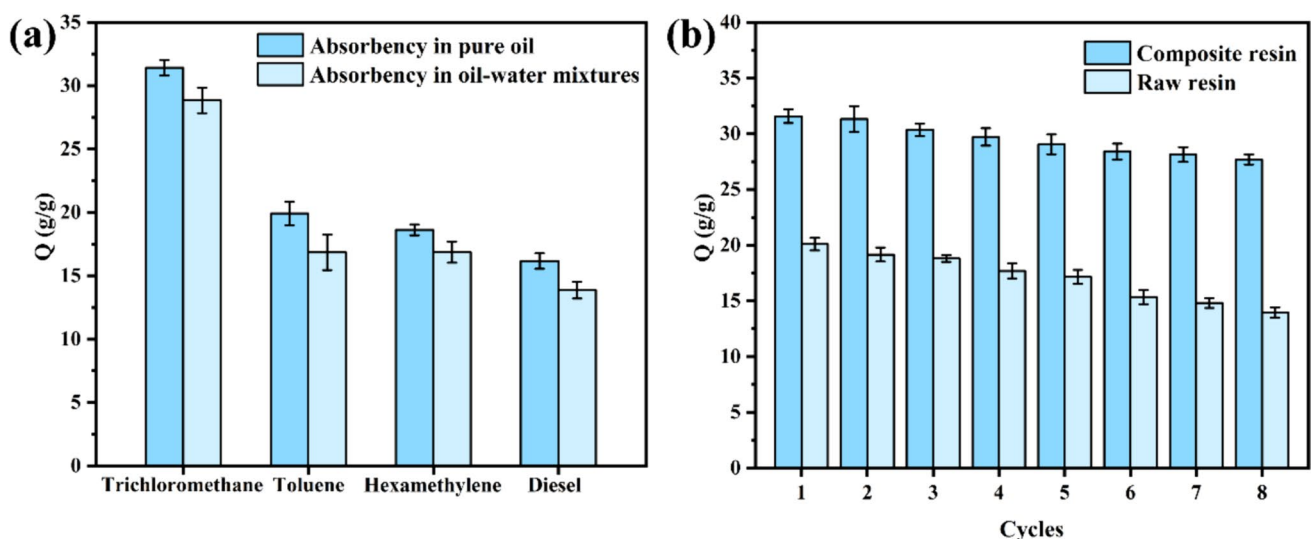

Fig. 7 a Comparison of saturated oil absorbency of resin composite in pure oil and oil–water mixture; **b** regeneration properties of resin composite for trichloromethane

volume of the resin composite for oil absorption, providing more storage space, accelerating the oil absorption, and improving the life of the resin composite.

Conclusions

This study focuses on preparing a resin composite for oil absorption. CoAl-LDO nanoparticles were modified with β-CD and KH-570 to enhance oil uptake. Under the optimized addition amount of 2 wt% CoAl-LDO-ECD-KH, the composite achieved maximum capacities of 16.17–31.42 g/g for various test oils and exhibited good reusability. This could be attributed to the formation of more pore structures by β-CD macromolecules. In addition, cobalt-aluminum bimetallic oxide nanoparticles also participate in the construction of 3D network structure, increasing the strength of the resin composite. Kinetic studies indicated the resin composite followed a pseudo-second-order model. The selectivity tests showed high efficiency in oil–water mixtures. This paper proposes a universal strategy for the preparation of β-CD-modified metal oxide nanoparticle composite sorbents. The strategy can be used to treat various types of oil spills and has promising application prospects.

Data availability The data that support the findings of this study are available on request from the corresponding author.

Declarations

Conflict of interest The authors declare that they have no competing interests.

References

1. T. Zhang, Q. Zhang, X.P. Wang, Q.R. Li, J. Rong, F.X. Qiu, RSC Adv. **5**, 101186 (2015)
2. X.J. Yue, T. Zhang, D.Y. Yang, F.X. Qiu, J. Rong, J.C. Xu, J.S. Fang, Chem. Eng. J. **309**, 522 (2017)
3. T. Zhang, X.J. Yue, D.Y. Yang, Q. Guo, F.X. Qiu, Z.D. Li, Appl. Organomet. Chem. **32**, e4244 (2018)
4. S. Wolfram, J. Joël, K. Gessler, Chem. Rev. **98**, 1787 (1998)
5. Y.L. Chen, J.Q. Su, W.X. Dong, D.X. Xu, L. Cheng, L.K. Mao, Y.X. Gao, F. Yuan, Food Chem. **383**, 132605 (2022)
6. B.R. Tian, Y.M. Liu, J.Y. Liu, Carbohyd. Polym. **251**, 116871 (2021)
7. B.F. Zhao, L.Y. Jiang, Q. Jia, Chinese Chem. Lett. **33**, 11 (2022)
8. J. Liu, J. Zhou, Z.H. Wu, X. Tian, X.Y. An, Y. Zhang, G.S. Zhang, F.X. Deng, X.L. Meng, J.H. Qu, J. Hazard. Mater. **432**, 128758 (2022)
9. X. Li, T.T. Liu, F. Tian, X.Y. Tao, Z.S. Wu, Korean J. Chem. Eng. **39**, 2972 (2022)
10. R. Indranil, J.F. Stoddar, Accounts Chem. Res. **54**, 1440 (2021)
11. J.M. George, B. Mathew, Korean J. Chem. Eng. **38**, 624 (2021)
12. J.H. Qu, D. Ming, F.X. Bi, Y. Tao, L. Wang, Z. Jiang, G.S. Zhang, B. Zhang, Y. Zhang, J. Clean. Prod. **364**, 131165 (2022)
13. M. Hassan, R. Naidu, J.H. Du, F.J. Qi, M.A. Ahsan, Y.J. Liu, Int. J. Biol. Macromol. **207**, 826 (2022)
14. J.M. Ma, D.R. Wang, W. Zhang, X.Y. Wang, X. Ma, M.S. Liu, Q.L. Zhao, L.C. Zhou, S.X. Sun, Z.F. Ye, Process Biochem. **121**, 298 (2022)
15. W. Zhang, P. Sun, D.S. Liu, Q.L. Zhao, B.Z. Zou, L.C. Zhou, Z.F. Ye, J. Taiwan Inst. Chem. Eng. **119**, 286 (2021)
16. L. Ding, Y. Li, D. Jia, J.P. Deng, W.T. Yang, Carbohyd. Polym. **83**, 1990 (2011)
17. J. He, L. Ding, J.P. Deng, W.T. Yang, Polym. Adv. Technol. **23**, 810 (2012)
18. T.R. Thatiparti, D. Juric, A. Horst, Bioconjugate Chem. **28**, 1048 (2017)
19. G.Y. Zhu, Z.B. Xiao, R.J. Zhou, G.X. Zhu, Y.W. Niu, J. Incl. Phenom. Macro. **84**, 219 (2016)
20. N.N. Liu, Y.H. Wu, H.T. Sha, J. Colloid Interf. Sci. **516**, 98 (2018)
21. J.D. Dai, J.M. Pan, L.C. Xu, X.X. Li, Z.P. Zhou, R.X. Zhang, Y.S. Yan, J. Hazard. Mater. **205**, 179 (2012)
22. F.B. Liu, W.T. Zhang, W.J. Chen, J. Wang, Q.F. Yang, W.X. Zhu, J.L. Wang, Chem. Eng. J. **310**, 187 (2017)
23. P.N. Ashitha, S. Akhil, K.T. Varughese, J. Appl. Polym. Sci. **139**, 1 (2021)
24. C. Song, L. Ding, F. Yao, J.P. Deng, W.T. Yang, Carbohyd. Polym. **91**, 217 (2013)
25. S.X. Li, J.P. Wang, W.J. Qu, J.J. Cheng, Y.N. Lei, D. Wang, F. Zhang, Eur. Polym. J. **123**, 109412 (2020)
26. B.G. Godiya, S. Gabrielli, S. Materazzi, M.S. Pianesi, N. Stefanini, E. Marcantoni, J. Environ. Manag. **231**, 1012 (2019)
27. F. Tamaddon, E. Ahmadi-AhmadAbadi, J. Polym. Environ. **31**, 406 (2023)
28. T. Zhang, X.B. Xie, C. Zhang, D.Y. Yang, F.X. Qiu, Polym-Plast. Technol. **57**, 1665 (2018)
29. H.B. Wan, J. Jiang, Q.F. Xu, Y.Z. Zhou, X.G. Wang, M.M. Lv, D.Y. Chen, B. Zhang, J.M. Lu, Chem. Eng. Sci. **276**, 118832 (2023)
30. Q.Z. Liu, M.Q. Ye, G.Q. Yu, A.J. Han, J. Appl. Polym. Sci. **140**, e53429 (2023)
31. Y.S. Ho, G. Mckay, Water Res. **33**, 578 (1999)
32. Y.S. Ho, G. Mckay, Process Biochem. **34**, 451 (1999)
33. J.S. Park, C. Han, J.Y. Lee, S.D. Kim, J.S. Kim, J.H. Wee, Purif. Technol. **43**, 111 (2006)